Skin Friction Reduction in a Turbulent Boundary Layer with Miniature Vortex Generators

Kai Zhang, Jiayang Luo, Xiaohui Wei, and Yu Zhou

Abstract Motivated by the substantial drag reduction of Plasma-generated streamwise vortices (Cheng et al. in Flat plate drag reduction using plasma-generated streamwise vortices. J Fluid Mech 918, 1), this study explores the feasibility of using one array of miniature vortex generators (MVGs) to reduce the skin-friction in a turbulence boundary layers (TBL). Various MVG arrays, amount to a total of 486, are examined, including different MVG shapes, height, induced angle and transverse spacing. The skin friction is measured using a high-resolution floating element (FE) force balance. It has been found for the first time experimentally that one array of simple triangle shape MVGs may achieve a drag reduction (DR) up to 4.3% at a momentum-thickness-based Reynolds number of $Re_\theta = 14{,}800$. This DR exhibits a strong dependence on the MVG height, induced angle and transverse spacing. With the ease to implement such a simple device in practice, this finding opens opportunities for a wide arrange of engineering applications.

Keywords Drag reduction · Vortex generator · Turbulence boundary layer

1 Introduction

In this paper, we present an exploration on the drag reduction (DR) in turbulence boundary layers (TBLs) over a flat plate using miniature vortex generators (MVGs). Vortex generators were widely used to control the flow separation on the suction side of poor aerodynamic surfaces or in strong adverse pressure gradients [2–4]. Researchers are also interested in using sub-boundary layer MVGs (usually 0.1–1 δ) to stabilize the Tollmien-Schlichting waves and postpone the turbulence transition [5, 6]. Recently, plasma vortex generators were used to produce large-scale streamwise

K. Zhang · J. Luo · X. Wei · Y. Zhou (✉)
Center for Turbulence Control, Harbin Institute of Technology (Shenzhen), Shenzhen 518055, China
e-mail: yuzhou@hit.edu.cn

K. Zhang
e-mail: zhangkai2021@hit.edu.cn

© The Author(s), under exclusive license to Springer Nature Singapore Pte Ltd. 2024

D. Kim et al. (eds.), *Fluid-Structure-Sound Interactions and Control*, Lecture Notes in Mechanical Engineering, https://doi.org/10.1007/978-981-97-6211-8_5

vortices (LSSVs), which could stabilize the quasi-streamwise vortices (QSVs) and reduce the drag in TBL beyond 70% [1, 7]. Thomas et al. [8] used plasma actuators and achieved net energy savings in TBL with Re_θ up to 18,500, which demonstrates the possibility of using LSSVs to reduce skin friction in the engineering level. One interesting question arises. Could the MVGs be deployed for skin friction reduction in a TBL? It is well known that MVGs can generate streamwise vortices up to 50 times their height, which is comparable with the length scale of the QSV. Furthermore, in the TBL, the tip flow speed of an MVG is high enough to form a strong vortex. For instance, Foster and White [9] reported that the tip speed of a $h = 0.2\delta$ MVG is 75% of the free stream velocity. Chan and Chin [10, 11] performed a well-resolved large eddy simulation to investigate the influence of miniature vortex generators on the large-scale motions in a TBL. They find a drag reduction of up to 2% in the near downstream flow following the MVG. However, until now, there is no experimental evidence to demonstrate the DR capability by using MVG arrays.

In summary, the first objective of this investigation aims to explore the feasibility of using MVGs to achieve drag reduction in turbulence boundary layers. The current work will also perform a comprehensive experimental study to disclose the influence of the MVG's parameters on DR, including the MVG height, induced angle, transverse spacing and Reynolds number.

2 Experimental Setup

Experiments were performed in a close circuit low-speed wind tunnel that has a Plexiglas test section with a dimension of 560 × 80 × 100 cm ($L \times W \times H$). As shown in Fig. 1, a flat plate with a dimension of 500 × 260 mm (L × W) was flush mounted at the bottom of the test section. The free stream velocity U_∞ varied between 20 m/s to 40 m/s during the test. The test plate was 3D-printed using a rapid prototyping machine and embedded into an aluminum frame to precisely control the dimensions of the test plate. The skin friction was measured using a floating-element (FE) force balance built in house. The used force balance was substantially revised from the previously developed FE force balance [1]. Two air flotation decks were used to make the floating element frictionless and constrict the non-streamwise motions of the test element. The direct skin friction was further amplified by two times using a lever mechanism. The gap between the floating-element and the bottom wall of test section was reduced to 0.2 mm to minimize the measurement error. The new design FE force balance has a resolution of 10^{-4} N and the minimum skin friction tested was 0.12 N under free stream velocity $U_\infty = 20$m/s. The measurement uncertainty is within 2% of the minimum measured skin friction.

To make this investigation simple, co-rotation, triangle shape MVGs were used. These MVGs were tiny stainless-steel plates inserted into the floating element and separated into four rows to fully take advantage of the LSSVs. The streamwise separation distance between these two MVG rows was 100 mm. The MVG arrays were mounted at 3.5 m downstream of the tunnel contraction section. The momentum

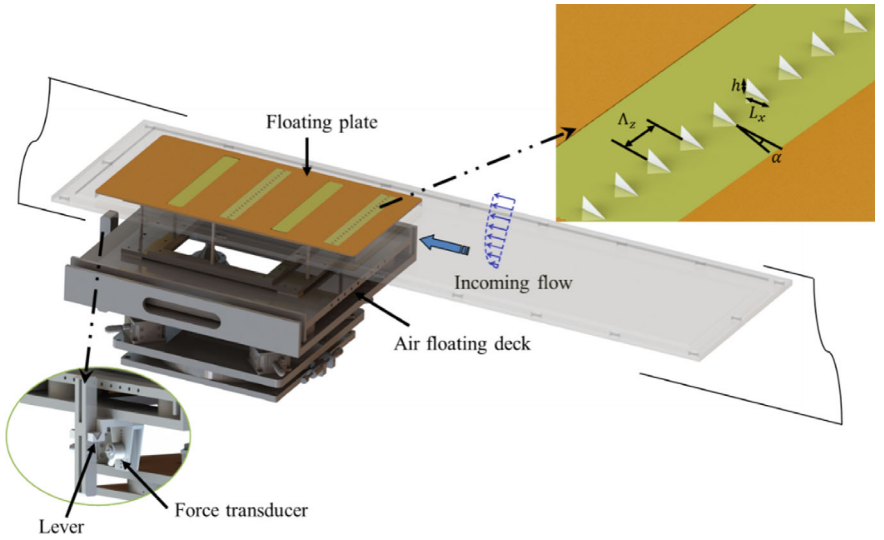

Fig. 1 Schematic of experimental setup. The MVGs are inserted into a floating plate. The skin friction is directly measured using a specially designed high-resolution force balance

thickness Reynolds number was $Re_\theta = 8500$ to 14,800 at the test location. The locally generated TBL had been fully characterized, and detailed information, including boundary layer thickness δ, viscous lengthscale δ_ν, friction velocity u_τ and Re_τ can be found in Zhang et al. [12] The height of the MVG array could be adjusted by a lab jack. Several MVG heights, transverse spacing, and induced angles of attack were tested. One row and two raws (separate distance 200 mm) and four rows of MVG arrays were examined as well. A total amount of 486 MVG configurations were evaluated. Detailed parameters of the MVG and the characteristics of the uncontrolled TBL can be found in Table 1. In Table 1, h is the height of the MVG, Λ_z is the transverse spacing between MVG plates, L_x/h is the aspect ratio of the MVG, and δ^* is the displacement boundary layer thickness.

Table 1 Boundary layer and MVGs parameters

U_∞ (m/s)	Re_θ	Re_τ	h/δ^*	Λ_z/h	L_x/h	α (○)
20, 30, 40	8500–14,800	3300–5500	0.2–1.0	5–15	2.5	10, 15, 20

3 Results and Discussion

Although we examined a huge amount of MVG configurations, to make the paper concise, in the following content, we only present the most persuasive results. Figure 2 shows the dependence of DR on MVG configurations at $Re_\theta = 14800$. . The parameters investigated are MVG height (Fig. 2a), MVG induced angle (Fig. 2b) and MVG transverse spacing (Fig. 2c). The DR rate is directly presented as the drag variation $\Delta F = \left(F_{MVG} - F_{ref}\right)/F_{ref}$, where F_{MVG} is the skin friction on the FE with an MVG array and F_{ref} is the skin friction on the FE without MVG (flat plate). DR is widely observed for many MVG configurations according to force measurements. For all the test cases, a maximum DR of 4.3% is obtained for $h = 0.2\delta^*, \alpha = 10°, \Lambda_z/h = 5$ MVG configuration.

As shown in Fig. 2a, given the same transverse spacing Λ_Z and same induced angle, the skin friction is essentially increased for $h/\delta^* = 0.5$, but DR is achieved for $h/\delta^* \leq 0.2$. The optimized MVG height is $h/\delta^* = 0.2$, but the DR is close to each other for $h/\delta^* = 0.2$ and $h/\delta^* = 0.1$ cases. Besides generating LSSVs, MVGs will induce an extra shape drag at the same time. The DR is the consequence of the balance between the drag reduction by stabilizing QSVs in TBL and the MVGs' shape drag. Increasing MVG height will considerably strengthen the LSSVs because the MVG tip speed increases significantly with MVG height in TBL, especially in the inner layer of TBL. As a result, DR is detected for $h/\delta^* = 0.1$. However, the MVG shape drag will remarkably rise with h as well. As the TBL velocity increases exponentially with vertical wall distance, the increment of the LSSV strength decreases with MVG height. As a result, the optimal MVG height is $h/\delta^* = 0.2$ in this experiment.

Figure 2b displays the impacts of induced angle on DR. DR is monotonically decreasing with α. This is due to the shape drag will considerably increasing with induced angle. However, for the same MVG height, the strength of LSSVs is not expected to be enhanced much. The dependence of DR on transverse spacing is shown in Fig. 2c. The results indicate that more MVG inserts will lead to more DR. The size of the generated LSSVs is on the same order of the MVG height. Thus, LSSVs will not interact with each other at $\Lambda_z/h = 5$. Therefore, the strength of the LSSVs is linearly proportional to the number of MVG inserts in the current setup. Wei et al. [7] discovered that DR is proportional to the strength of LSSVs. The measurement results shown in Fig. 2c can be expected.

Figure 3 shows the influence of the induced angle and transverse spacing on DR together. The induced angle and the transverse spacing are the abscissa and ordinate of Fig. 3, respectively. Figure 3 confirms the observations concluded from Fig. 2. The higher DR range is located at the bottom-left corner of the figure, and the DR is, in general, monotonically decreased with transverse spacing and induced angle.

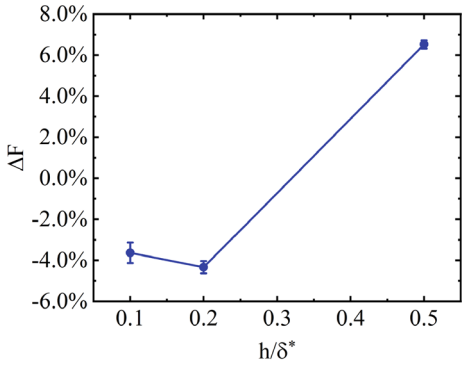

(a)$\Lambda_z/\mathrm{h} = 5, \alpha = 10^{\circ}$

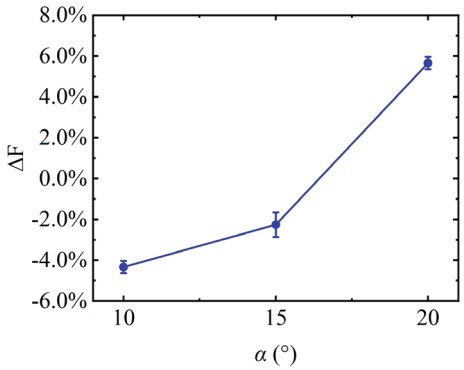

(b) $\Lambda_z/\mathrm{h} = 5, h/\delta^* = 0.2$

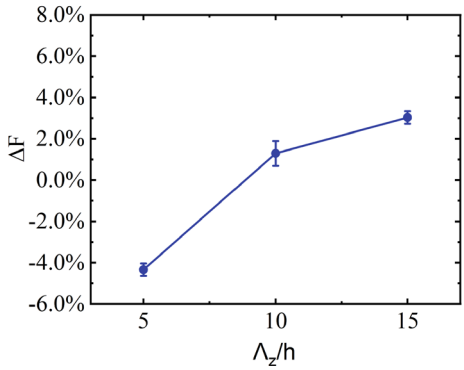

(c) $h/\delta^* = 0.2, \alpha = 10^{\circ}$

Fig. 2 Drag reduction rate under different test cases. **a** Influence of MVG height on DR. **b** Influence of induced angle on DR. **c** Influence of transverse spacing on DR. These results are at the highest tested Reynolds number Re_θ=14,800. Each case was repeated five times, and the mean DR is plotted

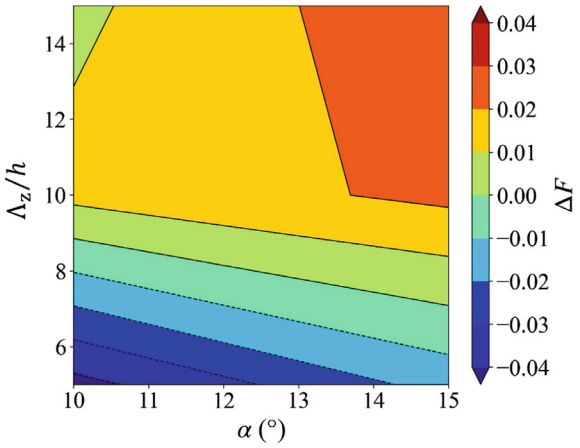

Fig. 3 Influence of transverse spacing and induced angle on DR

4 Conclusion

The current study demonstrates the feasibility of using MVG arrays to reduce skin friction in TBLs at Reynolds number up to $Re_\theta = 14800$. MVG with a height scale less than the displacement thickness of a boundary layer could generate strong enough LSSVs to stabilize the QSVs, meanwhile limiting the shape drag of MVG itself. A comprehensive experimental study is performed to evaluate the impact of MVG parameters on DR effect. A high-resolution FE balance is used to directly measure the skin friction. 486 combinations of MVG heights, induced angles, transverse spacings and Reynolds numbers are tested. DR is detected for a wide range of MVG configurations, which proves MVG is an effective way to reduce skin friction in TBLs. The force measurement results show DR is inversely proportional to MVG height, induced angle and transverse spacing. A maximum DR of 4.3% is achieved.

Acknowledgements KZ wishes to acknowledge support from NSFC through Grant 12202125 and from the Guangdong Basic and Applied Basic Research Foundation through Grant 2023A1515011269

References

1. Cheng XQ, Wong CW, Hussain F, Schröder W, Zhou Y (2021) Flat plate drag reduction using plasma-generated streamwise vortices. J Fluid Mech 918
2. Godard G, Stanislas M (2006) Control of a decelerating boundary layer. Part 1: optimization of passive vortex generators. Aerosp Sci Technol 10:181–191
3. Godard G, Foucaut J-M, Stanislas M (2006) Control of a decelerating boundary layer. Part 2: optimization of slotted jets vortex generators. Aerosp Sci Technol 10:394–400
4. Von Stillfried F, Wallin S, Johansson AV (2011) Evaluation of a vortex generator model in adverse pressure gradient boundary layers. AIAA J 49:982–993

5. Shahinfar S, Fransson JHM, Sattarzadeh SS, Talamelli A (2013) Scaling of streamwise boundary layer streaks and their ability to reduce skin-friction drag. J Fluid Mech 733:1–32
6. Fransson JHM (2015) Transition to turbulence delay using a passive flow control strategy. Procedia IUTAM 14:385–393
7. Wei X, Zhou Y (2023) Dependence on Reynolds number of skin-friction reduction using plasma-generated streamwise vortice. In: 6th symposium of fluid-structure-sound interactions and control
8. Thomas FO, Corke TC, Duong A, Midya S, Yates K (2019) Turbulent drag reduction using pulsed-DC plasma actuation. J Phys D Appl Phys 52:434001
9. Forster KJ, White TR (2014) Numerical investigation into vortex generators on heavily cambered wings. AIAA J 52:1059–1071
10. Chan CI, Chin RC (2022) Investigation of the influence of miniature vortex generators on the large-scale motions of a turbulent boundary layer. J Fluid Mech 932:A29
11. Chan CI, Chin RC (2022) Decomposition of the Reynolds shear stress in a turbulent boundary layer modified by miniature vortex generators. Phys Rev Fluids 7:54603
12. Zhang X, Wei X, Wang HF, Yao SB (2022) Active skin-friction reduction in the turbulent boundary layer of high Reynolds numbers. In: 23rd Australasian fluid mechanics conference